

Supported metallocene catalysis as an efficient tool for the preparation of polyethylene/carbon nanotube nanocomposites: effect of the catalytic system on the coating morphology†

Daniel Bonduel,^{ab} Stéphane Bredeau,^a Michäel Alexandre,^c Fabien Monteverde^c and Philippe Dubois^{*ac}

Received 5th February 2007, Accepted 9th March 2007

First published as an Advance Article on the web 29th March 2007

DOI: 10.1039/b701764b

Homogeneous or periodical surface coating of multiwalled carbon nanotubes (MWNTs) can be achieved by *in situ* polymerization of ethylene as catalyzed directly from the nanotube surface-treated by a highly active metallocene-based complex, *e.g.*, Cp*₂ZrCl₂/methylaluminoxane. This polyethylene (PE) coating allows for the break-up of the native nanotube bundles. Immobilization of methylaluminoxane onto the surface of the carbon nanotubes was evidenced by scanning electron microscopy (SEM) and confirmed by X-ray photoelectron microscopy (XPS) and time-of-flight secondary ion mass spectrometry (TOF-SIMS). The thermal behaviour and degradation were studied by means of differential scanning calorimetry (DSC) and thermogravimetric analysis (TGA). Transmission electron microscopy (TEM) was used to image polymer-coated MWNTs, showing either a relatively smooth or a textured polymer coating present on the surface of individual, debundled nanotubes, *i.e.*, PE/MWNT nanohybrid “sausage”-like or “shish-kebab”-like structures, respectively. It was clearly demonstrated that by modifying the design of the catalytic complexes, it was possible to tune by a reproducible way the morphology of the PE coating around the MWNTs.

Introduction

Since the discovery of carbon nanotubes (CNTs) by Ijima,¹ their unique mechanical and electrical properties have attracted intense theoretical and experimental attention from both academics and industrials. Treacy *et al.*² determined the Young's modulus of isolated CNT by measuring the amplitude of its intrinsic thermal vibrations and found that its average Young's modulus reaches 1.8 TPa. Wong *et al.*³ used an atomic force microscope to determine the mechanical properties of multiwalled carbon nanotubes (MWNTs) and found that they are characterized by a very high toughness. Therefore, among numerous potential applications of carbon nanotubes, their use as reinforcing materials for polymers has recently received considerable attention.^{4–7} The incorporation of MWNTs in polymers is envisaged to produce structural materials with dramatically improved modulus and strength. However, preparation of nanocomposites with CNTs homogeneously dispersed within a polymer matrix is a technical challenge since this kind of one-dimensional nanofiller shows a trend to form aggregates owing to very strong and numerous π - π interactions as well as a high density of entanglements.

Therefore, the successful development of CNT/polymer composites depends to a large extent on the ability to disperse the CNTs homogeneously in the polymer matrices and to ensure strong CNT-polymer interfacial adhesion for good load transfer. A variety of methods have been used to help the dispersion of CNTs in polymer matrices and/or improve load transfer *via* physical, chemical, or combined approaches.⁸ One can cite surfactant-assisted dispersion,⁹ high power sonication,¹⁰ *in situ* polymerization,¹¹ electric- or magnetic-field-induced alignment of nanotubes,^{12,13} plasma polymerization,¹⁴ and surface modification such as inorganic coating,¹⁵ polymer wrapping,¹⁶ as well as protein functionalization.¹⁷ Nevertheless, developing a much softer and more efficient method able to break down carbon nanotube bundles remains very important for the development of the ultimate nanocomposites.

Recently, we have reported in a preliminary communication¹⁸ an original method which relies upon the *in situ* polymerization of ethylene catalyzed by a highly active metallocene/methylaluminoxane (MAO) complex physico-chemically anchored onto the carbon nanotube surface. As a result, carbon nanotubes are homogeneously coated by the *in situ* grown polyethylene (PE) chains, finally leading to the destructure of the nanotube bundles. The method used is derived from the polymerization-filling technique (PFT) initially investigated in Ziegler-Natta polymerization^{19,20} and more recently developed for metallocene catalysis applied to a broad range of microfillers such as kaolin, silica, wollastonite, and graphite.^{21–24}

Therefore, the purpose of this study is to complement our previous effort¹⁸ by providing insight into the anchoring of MAO at the nanotube surface, the fixation of the catalyst

^aLaboratory of Polymeric and Composite Materials, University of Mons-Hainaut, Place du Parc 20, 7000 Mons, Belgium.

E-mail: philippe.dubois@umh.ac.be; Fax: +32 65 37 34 84; Tel: +32 65 37 34 80

^bNanocyl S. A., Rue de l'Essor 4, 5060 Sambreville, Belgium

^cMateria Nova Research Centre, av. N. Copernic 1, 7000 Mons, Belgium

† Electronic supplementary information (ESI) available: X-ray photoelectron spectroscopy (XPS): analysis of neat MWNTs, MAO-treated MWNTs, and MAO/Cp*₂ZrCl₂-treated MWNTs. See DOI: 10.1039/b701764b

(i. e., Cp*₂ZrCl₂) onto the surface-activated carbon nanotubes, and the *in situ* polymerization of ethylene leading to the coating of carbon nanotubes and finally to the deconstruction of the nanotube bundles upon further melt blending within any polymer matrix. Moreover, more attention has been paid to the investigation of the influence of the used catalytic system (catalyst + cocatalyst) on the coating morphology through the characterization of the extent of polyethylene coating around the nanotubes, essentially by TEM analyses. The thermal properties of the corresponding composites, studied by DSC and TGA analyses, are also reported here. It is worth pointing out that very recently, Funck and Kaminsky interestingly have reported on the possibility to polymerize propylene from CNTs by also using a metallocene/MAO catalytic system. In their study, the MAO cocatalyst proved to be covalently bound onto the surface of oxidized carbon nanotubes²⁵ resulting in a better CNT/matrix interfacial adhesion.

Experimental

Materials

All air- and moisture-sensitive compounds (e.g., catalyst and cocatalyst) were manipulated using standard vacuum line, Schlenk, or cannula techniques under dry nitrogen or in a glovebox under a deoxygenated and dry nitrogen atmosphere (O₂ and H₂O < 1 ppm). n-Heptane was dried and stored over 4 Å molecular sieves while toluene was refluxed over CaH₂ and freshly distilled prior to use under N₂ atmosphere. Bis(pentamethyl-η⁵-cyclopentadienyl)zirconium(IV) dichloride (Cp*₂ZrCl₂) was purchased from Aldrich, used without further purification, and then stored at 4 °C as a stock solution in toluene or in n-heptane with a known concentration (5.2 mM or 0.8 mM, respectively). MMAO-3A (7.0 wt% solution in n-heptane; MMAO-3A is a modified methylaluminoxane with isobutyl groups, CH₃/i-C₄H₉ ~ 2.3) was purchased from AkzoNobel and used as received. MAO (30 wt% solution in toluene) was kindly supplied by Total Petrochemicals Research Feluy (Belgium), and diluted in dried toluene with a known concentration (1.31 M). Ethylene (Air Liquide, 99.95%) was used without further purification. The purified multiwalled carbon nanotubes (MWNTs) were kindly supplied by Nanocyl S.A. and were previously dried at 105 °C under reduced pressure (10⁻² mmHg) for 8 hours and then stored under N₂ atmosphere. The polymerization reactions were performed in a glass reactor by following the ethylene consumption with a Zipperclave Batch Reactant Gas Delivery System (BRGDS).

Representative procedure for polymerization

i) Carbon nanotube surface activation. A 250 mL polymerization flask was filled with 0.25 g of MWNTs and flame-dried under high vacuum. The flask was then filled with nitrogen and placed in an oil bath at 40 or 50 °C. 20 ml of dried and deoxygenated n-heptane and 0.75 ml of MMAO-3A (1.90 M) or 1.10 mL of MAO (1.31 M) were added under nitrogen. The MWNTs in contact with the aluminoxane were stirred for 1 h at 40 (MMAO-3A) or 50 °C (MAO). Solvents were then distilled off at 50 °C under reduced pressure. The

solvents, together with any volatile organoaluminium compounds were trapped in a flask cooled by liquid nitrogen for aluminium titration. Treated MWNTs were further heated at 150 °C under reduced pressure for 90 min.

ii) Polymerization step. The polymerization reactions were performed in a 250 mL glass reactor by following the ethylene consumption with a BRGDS device. The aluminoxane-treated MWNTs were dispersed in 20 ml dried n-heptane. Then, 0.80 ml of Cp*₂ZrCl₂ (4.1 μmol in Zr, [Al]/[Zr] = 350) was added to the suspension. The stirred mixture was then heated to 50 °C for 15 min. The reactor was purged by ethylene (0.5 min) in order to remove nitrogen. The polymerization reaction was carried out under a constant pressure of 2.7 bars of ethylene at 50 °C and vigorous stirring for a defined period of time. The final material was precipitated in 200 ml methanol acidified with hydrochloric acid and filtered off. The resulting material was then dried at 60 °C for ca. 12 h in a ventilated oven.

Characterization

Differential scanning calorimetry (DSC) was carried out using a Q 100-TA Instrument under nitrogen atmosphere. Samples (5–10 mg) were analyzed by first heating the sample from 55 to 160 °C at 10 °C min⁻¹, then cooling from 160 to 55 °C at 10 °C min⁻¹ and heating it again from 55 to 160 °C at 10 °C min⁻¹. Results of the second heating run were used for interpretation. Thermogravimetric analysis (TGA) was carried out using a Q 50-TA Instrument under a helium or air atmosphere. The measurement consisted of heating the sample from 30 to 850 °C at 20 °C min⁻¹ under helium flow or from 30 to 950 °C at 20 °C min⁻¹ under air flow. Surface analysis of the MWNTs (pure and surface-treated) was carried out by X-ray photoelectron spectroscopy (XPS) (Thermo VG scientific, VG ESCALAB 220iXL) and time-of-flight secondary ion mass spectrometry (TOF-SIMS) (Ion Tof, ToF-SIMS IV). The morphology of the MWNTs (pure, surface-treated and PE-coated) was evaluated by scanning electron microscopy (SEM) (Philips XL 20) connected with an EDS (EDAX) detector and by transmission electron microscopy (TEM) (Philips CM 200 at 120 kV).

Results and discussion

The polymerization-filling technique (PFT) applied for coating CNTs by polyethylene (PE) can be described as a four-step process: (i) anchoring methylaluminoxane (MAO), a commonly-used cocatalyst in metallocene-based olefin polymerization, onto the CNT surface, (ii) addition of the metallocene catalyst onto the surface-activated CNT, (iii) polymerization of ethylene onto the CNT surface, (iv) precipitation of PE onto the CNTs leading to their coating. This method leads finally to the break-up of the CNT bundles and to the efficient deagglomeration of the nanotubes upon melt blending within any polymer matrix.¹⁸ However, to the best of our knowledge, no evidence concerning the anchoring of methylaluminoxane onto the CNT surface and the fixation of the catalyst has been reported up to now.

Under the PFT experimental conditions, the MWNTs were first treated with MAO by reaction in n-heptane at 50 °C for

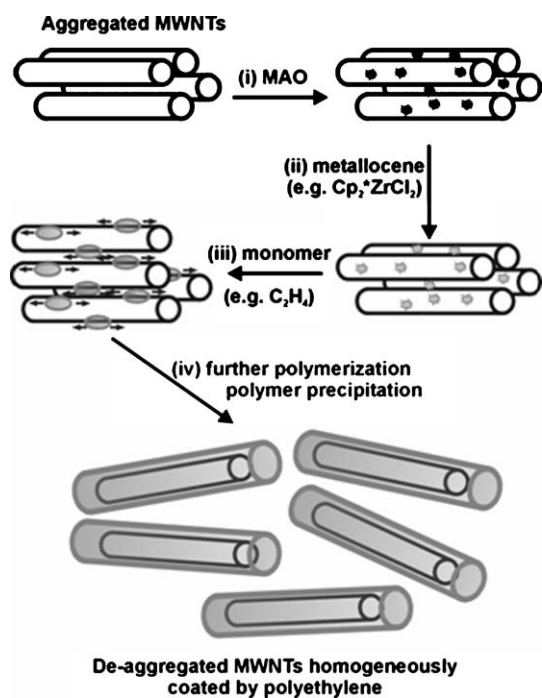


Fig. 1 Scheme of the polymerization-filling technique (PFT) applied to carbon nanotubes. MAO stands for methylaluminoxane and $\text{Cp}^*_2\text{ZrCl}_2$ for bis(pentamethyl- η^5 -cyclopentadienyl)zirconium(IV) dichloride.

1 hour, then for 90 minutes at 150 °C, after solvent evacuation (step i, Fig. 1).

The colorimetric titration of the alkylaluminium residues left after MWNT washing by hot toluene allowed the actual amount of aluminium immobilized onto the carbon nanotubes surface to be estimated. The experimental value (23.6×10^{-3} mol of Al per g of MWNT) showed that a large amount of MAO could be fixed onto the MWNTs. This large amount of immobilized MAO might arise from the high specific surface displayed by MWNTs coupled to possible interactions between the Lewis acid Al centers of MAO and the electron-rich surface of carbon nanotubes. In order to gain better insight into the interaction of the catalytic system with the MWNTs, the MAO deposition (and distribution) on the MAO-treated carbon nanotube surface was examined by scanning electron microscopy (SEM) connected with an electron de-excitation X-ray (EDS) analyzer. SEM micrographs for the native MWNTs and MAO-treated MWNTs, representative of the overall material, are shown in Fig. 2a and b, respectively, and are very different. It is evident from Fig. 2a that the CNT surfaces are clean and smooth even if some oxygen is present on the carbon nanotube surfaces as evidenced by a thin peak detected at 0.50 keV. The maximum at 1.60 keV has been attributed to contamination by silicon grease used to seal the glassware vessels. As a rule, the EDS analysis in Fig. 2b confirms the presence of MAO spread out on the MWNT surface, since the sharp maxima observed in the EDS mapping are characteristic of the constitutive atoms of the aluminosilicate derivatives, *i.e.*, O and Al atoms at 0.55 and 1.5 keV, respectively. It has to be noted that, in contrast to SWNTs that form packed bundles over distances of several

tens of nm, MWNTs are characterized by less dense bundles of entangled nanotubes that permit MAO to reach the heart of the bundles when dispersed in *n*-heptane.

The chemical elements located at the surface of native and MAO-treated MWNTs were also evaluated using XPS analysis (see ESI†). The presence of carbon and oxygen atoms in the MWNTs, and carbon, oxygen and aluminium atoms in the MAO-treated MWNTs has been established. The C1s scan of the MWNTs showed the peak of the sp^2 carbons at 284.3 eV and oxygen (O1s) shows up at 532.6 eV (with a relative abundance of 97.8 and 2.2%, respectively). Furthermore, after the MAO addition, there is an extra peak at 76.3 eV, which corresponds to Al2p, whereas the intensity of oxygen (O1s) increases to 22.6%, arising from the presence of oxygen coming from the MAO molecules attached to the carbon nanotubes.

These MAO-treated carbon nanotubes were then placed in contact with the polymerization precatalyst ($\text{Cp}^*_2\text{ZrCl}_2$) to form the active polymerization species (step ii), that is to say the methylated cationic zirconium species ($\text{Cp}^*_2\text{ZrMe}^+$) by the known cationization mechanism. Catalytic species should therefore be immobilized in the vicinity of the nanotube surface by electrostatic interactions between the cationic Zr center and the surface-anchored MAO-based anion. As shown in Fig. 2c, the MWNTs surface-treated with both MAO and $\text{Cp}^*_2\text{ZrCl}_2$ appear in the SEM image as a bundle of carbon nanotubes very similar to the ones described in Fig. 2b. The EDS analysis still confirms the presence of MAO anchored on the MWNT surface but there is no clear evidence that zirconium is adsorbed onto the carbon nanotubes surface, even though a very small signal could be detected at 2.00 keV, the intensity of which is only slightly higher than the average background. XPS analysis was also performed but due to the small amount of catalyst present in the medium it was not possible to conclude if zirconium was effectively immobilized onto the MAO-treated surface. As a consequence, an analysis by time-of-flight secondary ion mass spectrometry (TOF-SIMS) was carried out. The TOF-SIMS spectrum (positive mode) is shown in Fig. 3. In addition to the presence of aluminium as alumina, zirconium was clearly evidenced in comparison with the relative intensities of the different isotopes of this element. It can therefore be concluded that the fixation of the catalytic system onto the surface of carbon nanotubes effectively takes place.

In order to probe the efficiency of this immobilized catalytic system in ethylene polymerization, a set of experiments were compared. To determine the influence of MWNTs on the catalytic polymerization, ethylene was polymerized either in the absence of MWNTs, in the presence of MWNTs or after supporting the catalytic system on MWNTs. The corresponding polymerization kinetics, reported in a preliminary communication,¹⁸ have shown on one hand that non-treated MWNTs act as “spectators” in the polymerization and consequently do not perturb the course of ethylene polymerization. On the other hand, supporting the metallocene catalyst on the nanotubes by PFT increases significantly the efficiency of the polyethylene synthesis in solution. A boost in ethylene consumption has been clearly observed (the quantity of consumed C_2H_4 is by 28% more important than for the ethylene polymerization in the absence of any filler) allowing

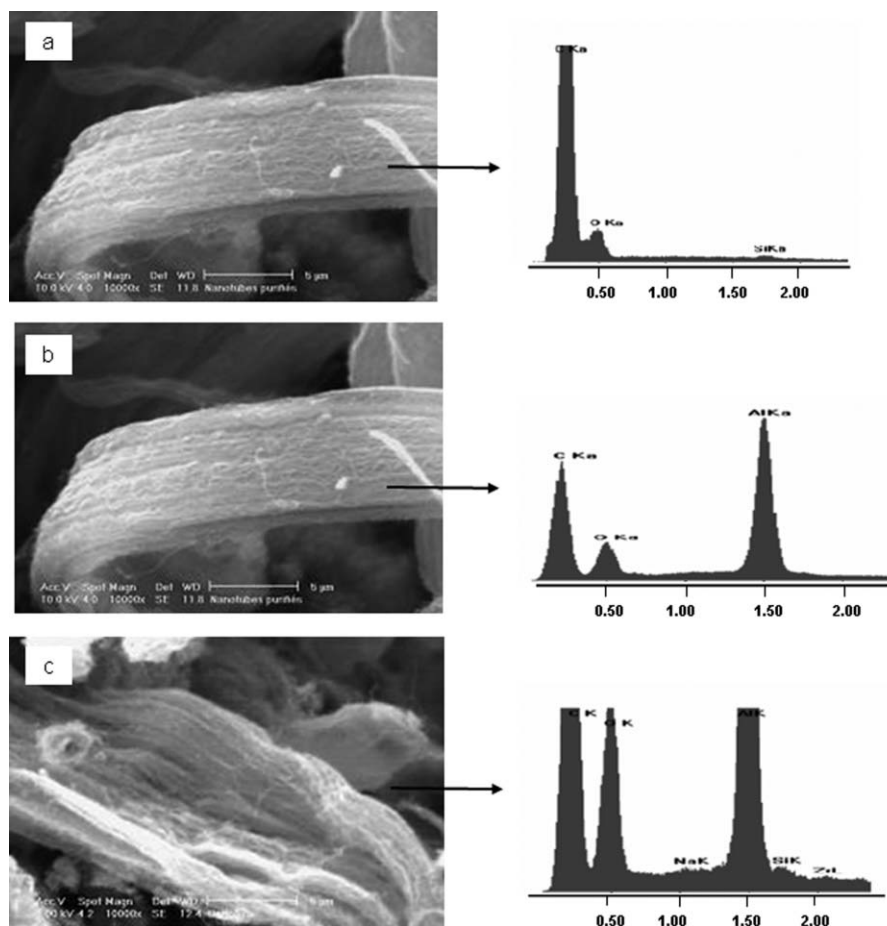


Fig. 2 SEM micrographs coupled with EDS analysis of (a) native MWNTs, (b) MWNTs treated with MAO and (c) MWNTs treated with MAO and $\text{Cp}^*_2\text{ZrCl}_2$.

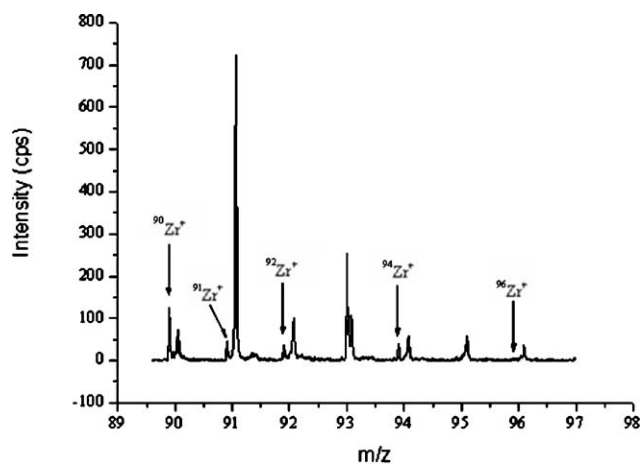


Fig. 3 TOF-SIMS spectrum (positive mode) of zirconium and respective isotopes of MWNTs treated with both MAO and $\text{Cp}^*_2\text{ZrCl}_2$.

the conclusion to be drawn that higher catalyst activities are measured for the surface-treated nanotubes when compared to homogeneous ethylene polymerization performed under the same experimental conditions. In the PFT, polyethylene is formed near the carbon nanotube surface. Because the chains are growing from the cationic species, the polymer is

exclusively formed in very close contact with the filler surface (step iii, Fig. 1) and, with increasing molecular masses, rapidly precipitates onto the CNTs to coat them and ultimately separate them from each other (step iv). To highlight the production of PE during this process, the composition and thermal characteristics of the polymerization-filled composites were determined by differential scanning calorimetry (DSC) as well as by thermogravimetric analysis (TGA). The melting temperatures of PE and PE-coated MWNT samples were determined by DSC from the second run. Interestingly, PE-coated MWNT displayed a T_m slightly lower than that of polyethylene obtained in the absence of filler by about 2–4 °C but in the temperature range typical for HDPE (128–135 °C).²⁶ This characteristic feature could indicate that the crystallization of PE is adversely affected by the close vicinity of the carbon nanotubes surface since carbon nanotubes could be considered as a good nucleating agent.²⁷ TGA was used to determine the relative amount of grafted polymer in PE-coated MWNTs. The weight loss occurring around 480–510 °C under helium may be assigned to the decomposition of the polyethylene. The analysis done under helium flow demonstrates that polyethylene in the composites is as thermally stable as polyethylene produced under the very same conditions but in the absence of filler. The shape of the decomposition curves is similar for all analyzed materials; the composites start to

degrade above 480 °C, in agreement with pure polyethylene which mainly degrades between 400 and 500 °C. This observation indicates that the degradation of PE in the composites is not really influenced by the MWNTs.

In order to characterize the extent of PE coating around the nanotubes, transmission electron microscopy (TEM) observation of MWNT-based composites containing 75 wt% of polyethylene was carried out and compared to pristine MWNTs (Fig. 4). The TEM image of pristine MWNTs (Fig. 4a) shows that the carbon nanotubes are piled up forming large bundles and ropes. In order to avoid compaction during HDPE-coated MWNT filtering and drying, TEM samples were directly taken from the polymerization suspension and deposited onto the TEM grid. For HDPE-coated MWNTs (Fig. 4b), one can observe typically two single long MWNTs completely separated from the starting bundle and homogeneously covered by a polyethylene layer (determination of coating diameter is about 32 nm in comparison with MWNT diameter of 8 nm), allowing the conclusion to be drawn that PFT is quite efficient at dissociating the MWNT bundles and individually coating the separated nanotubes with a thin layer of HDPE. A mechanism for this original homogeneous coating has already been published by some of us elsewhere²⁸ and proceeds in three steps. First, polymerization starts from catalyst spots anchored on the MWNT surface and produces patches of PE near the catalyst spots, arising from fast PE precipitation under the synthesis conditions. In a second stage, under continuous feeding of ethylene, the PE patches grow and slide along the MWNT surface to form PE sleeves. Finally, the PE sleeves join together to form a continuous and homogeneous PE coating around the carbon nanotubes.

In a further step, the influence of various factors (*i.e.*, cocatalyst, and temperature) on the morphology of the PE coating was studied. The polymerization-filling technique that was used to produce PE/MWNT nanohybrid with a continuous and relatively smooth coating ("sausage"-like

structure) was modified by first replacing conventional MAO by MMAO-3A (MMAO-3A is a modified methylaluminoxane with isobutyl groups, $\text{CH}_3/i\text{-C}_4\text{H}_9 \sim 2.3$). MMAO-3A was chosen for its higher solubility in *n*-heptane (MAO readily precipitates in *n*-heptane), allowing for more homogeneous anchoring of the cocatalyst in the first stage of MWNT treatment. After MMAO-3A anchoring and addition of the zirconium catalyst, high ethylene polymerization activities were detected for the surface-treated nanotubes, with the larger increase (by 125% for MMAO-3A/Cp*₂ZrCl₂-treated MWNTs) when compared to homogeneous ethylene polymerization carried out using MMAO-3A as a cocatalyst, under the same experimental conditions.

In order to gain more insight in the course of ethylene polymerization and to characterize MWNTs coated by different amounts of PE, ethylene polymerization supported on MWNTs was carried out in an experiment where samples were picked out consecutively every time 0.3 bar ethylene was consumed. Composition and thermal characteristics of the recovered MWNT/PE samples are given in Table 1. As expected, the successively recovered samples are characterized by an increased relative content of PE as determined by thermogravimetric analysis. These samples are also characterized by an increase of melting temperature and crystallinity with the amount of PE formed. This can be rationalized by the immobilization of the polymer chains on the surface of the treated MWNT and/or by their physical entanglement around the filler which results in limitation for the chain crystallization and defects in the crystalline structure, as already observed for PFT on graphite.²⁴ When the amount of PE increases, a smaller relative amount of polyolefinic chains remains in close contact with the nanotube surface and their overall crystallization is therefore favored. This effect is further confirmed by the values of W_c in Table 1, which are relatively independent of the polyethylene content above 30 wt% (*ca.* 65%) while a low degree of crystallinity is measured (30%) for the lower PE content (12%) (entry 1). It was not possible to isolate PE by dissolution in 1,2,4-trichlorobenzene at 140 °C for SEC analysis, due to gel formation. Therefore no information about molar masses that could give insights about the thermal behavior of the material could be obtained. Such a phenomenon was already reported in the case of polyethylene-layered

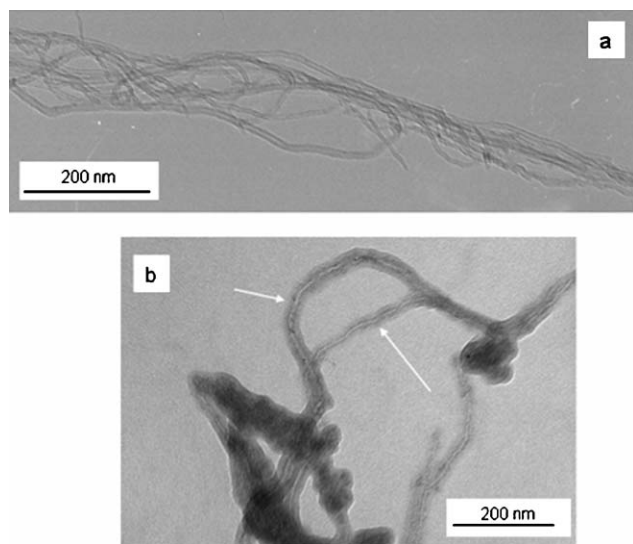


Fig. 4 TEM micrographs: a) neat MWNTs, b) MWNTs coated with *in situ* grown polyethylene (indicated by the arrows, PE content = 75 wt%).

Table 1 PE content and thermal characteristics of successively picked-out PE/MWNT nanocomposite samples as produced using MMAO-3A as cocatalyst (polymerization conditions: 1 g MWNT dispersed in 140 ml *n*-heptane, 16.5 μmol Zr (g MWNT)⁻¹, [Al]/[Zr] = 370, pressure (ethylene) = 1.1 bar, polymerization temperature = 50 °C)

| Entry ^a | Recovered mass/g | PE content ^b (wt%) | T_m ^c /°C | W_c PE ^d (%) |
|--------------------|------------------|-------------------------------|------------------------|---------------------------|
| 1 | 0.40 | 12 | 122 | 30 |
| 2 | 0.44 | 35 | 130.5 | 63 |
| 3 | 0.65 | 52 | 132.5 | 68 |
| 4 | 0.70 | 71 | 135 | 66 |

^a Each sample was consecutively picked out when 0.3 bar ethylene was consumed. ^b As determined by thermogravimetric analysis (weight loss recorded under helium flow with a heating ramp of 10 °C min⁻¹). ^c T_m = melting temperature as determined by differential scanning calorimetry (2nd heating scan at 10 °C min⁻¹). ^d W_c PE = polyethylene crystallinity obtained from differential scanning calorimetry (2nd heating scan at 10 °C min⁻¹).

silicate nanocomposites prepared by the *in situ* intercalative polymerization of ethylene by PFT.²⁹ Further studies to explain this crystallisation phenomenon are currently under way.

The morphology of the recovered nanocomposites was studied by TEM and is shown in Fig. 5. When comparing the TEM images representative for the overall material and taken at the same magnification, it is evident from these micrographs that a PE layer, whose thickness increases with time, closely coats the carbon nanotubes. The morphology of this coating is dramatically modified, the MWNTs are in fact decorated with disc-shaped objects (arrows), corresponding to PE single-crystal lamellae (edge-on view), resulting in a new nanohybrid morphology (“shish-kebab”-like structures). The central shish is the carbon nanotube while the kebabs are formed by PE chains. Such a morphology has already been described by Li *et al.*³⁰ when using a controlled HDPE crystallization method from solution to obtain such periodically patterned polymeric materials on individual carbon nanotubes. Since in our process the polymer grows directly from the activated surface of the MWNTs, it can be postulated that epitaxial growth of PE on MWNTs and geometric confinement by the MWNTs both play a role. It should be noted that in Fig. 5, most of the kebabs are nearly perpendicular to the MWNT surface; this is probably because adopting this perpendicular orientation could enable the PE to grow into larger crystals. In parallel and oblique orientations, space confinement from the adjacent lamellar crystals might eventually prevent them from growing larger. Clearly, this morphology development arises from the anchoring of the two different types of cocatalyst (MAO or MMAO-3A) on the surface of the MWNTs, in particular their distribution on the surface of the MWNTs. No noticeable agglomeration was observed in any of the TEM micrographs, indicating that original MWNTs can be also separated into

individual tubes by the MMAO-3A/metallocene-induced polymerization. One can observe that using MMAO-3A as cocatalyst in ethylene polymerization leads to a new morphology of the PE coating allowing us to assume that this one is strongly dependent on the chemical composition of the cocatalyst and/or its anchoring mechanism.

In order to try to modulate the polymerization activity and the relative solubility of growing PE chains in the reaction medium (*i.e.*, n-heptane), the effect of the temperature on the course of the ethylene polymerization was also investigated by carrying out a series of ethylene polymerization reactions at various temperatures with MMAO-3A as cocatalyst. The PE content and thermal characteristics of PE/MWNT nanocomposites are summarized in Table 2. As an example, our catalytic-anchored system was able to yield 0.75 g of PE after 50 min at 0 °C (entry 1). Increasing the polymerization temperature to successively 20, 30, 40 and 50 °C improved the activity but did not affect dramatically the melting temperature and crystallinity of the formed PE. The DSC thermograms for the different samples confirm that the PE produced, as obtained by PFT, is typical of HDPE with a melting point range between 132 and 135 °C. The interaction of the matrix with the filler surface slightly perturbs the melting behavior. As already underlined, when the PE content exceeds 50 wt% the degree of crystallinity is quite stable (Table 2), the contribution of the immobilized polymer chains on the surface of the treated particles being minor compared to the total amount of PE. TEM analysis was conducted to investigate the morphology of the resulting composites. Typical TEM micrographs for three of the five samples obtained are shown in Fig. 6 and are quite similar. The “shish-kebab”-like structure of the PE-coating around the carbon nanotubes is retained, this result clearly indicates that the temperature does not affect the morphology of the PE coating. On the basis of these TEM results, it is

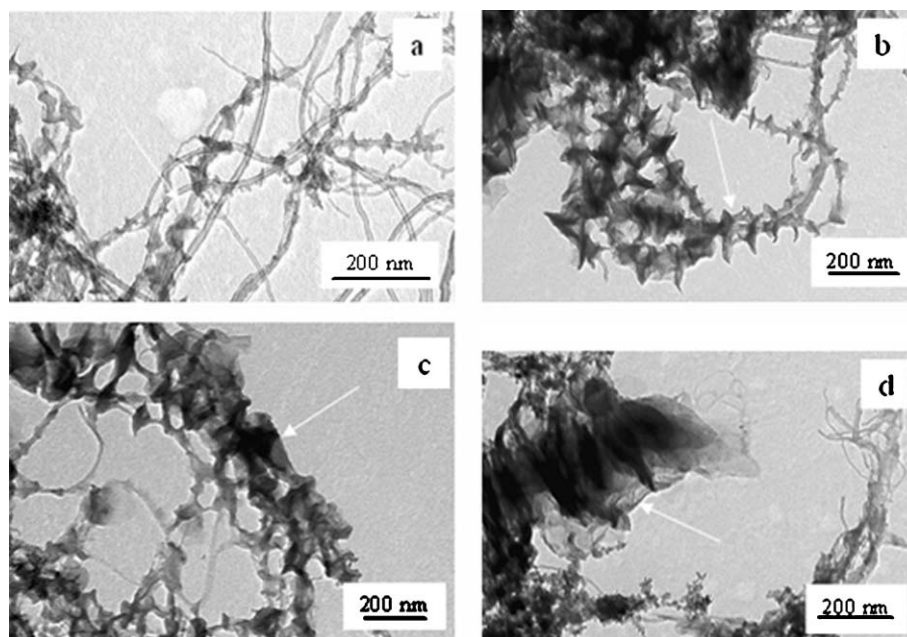


Fig. 5 TEM micrographs of PE-coated MWNTs as obtained by the polymerization-filling technique with 12 (a), 35 (b), 52 (c) and 71 wt% (d) PE respectively (see Table 1).

Table 2 PE content and thermal characteristics of PE/MWNT nanocomposites obtained at various temperatures using MMAO-3A as cocatalyst (polymerization conditions: 0.25 g MWNT dispersed in 40 ml n-heptane, 16.5 $\mu\text{mol Zr}$ (g MWNT)⁻¹, $[\text{Al}]/[\text{Zr}] = 350$, pressure (ethylene) = 1.3 bar)

| Entry | Polymerization temperature/ $^{\circ}\text{C}$ | Reaction time/min | Recovered mass/g | Activity ^a | PE content ^b (wt%) | T_m ^c / $^{\circ}\text{C}$ | W_c PE ^d (%) |
|-------|--|-------------------|------------------|-----------------------|-------------------------------|---|---------------------------|
| 1 | 0 | 51 | 1.00 | 41 | 68 | 133 | 52 |
| 2 | 20 | 22 | 0.75 | 64 | 59 | 135 | 52 |
| 3 | 30 | 8 | 0.88 | 220 | 67 | 133 | 63 |
| 4 | 40 | 4 | 0.97 | 155 | 60 | 132 | 54 |
| 5 | 50 | 4 | 1.21 | 269 | 76 | 134 | 56 |

^a Activity in $\text{kg} (\text{mol h bar})^{-1}$ of catalyst. ^b As determined by thermogravimetric analysis (weight loss recorded under helium flow with a heating ramp of $10\text{ }^{\circ}\text{C min}^{-1}$). ^c T_m = melting temperature as determined by differential scanning calorimetry (2nd heating scan at $10\text{ }^{\circ}\text{C min}^{-1}$). ^d W_c PE = polyethylene crystallinity obtained from differential scanning calorimetry (2nd heating scan at $10\text{ }^{\circ}\text{C min}^{-1}$).

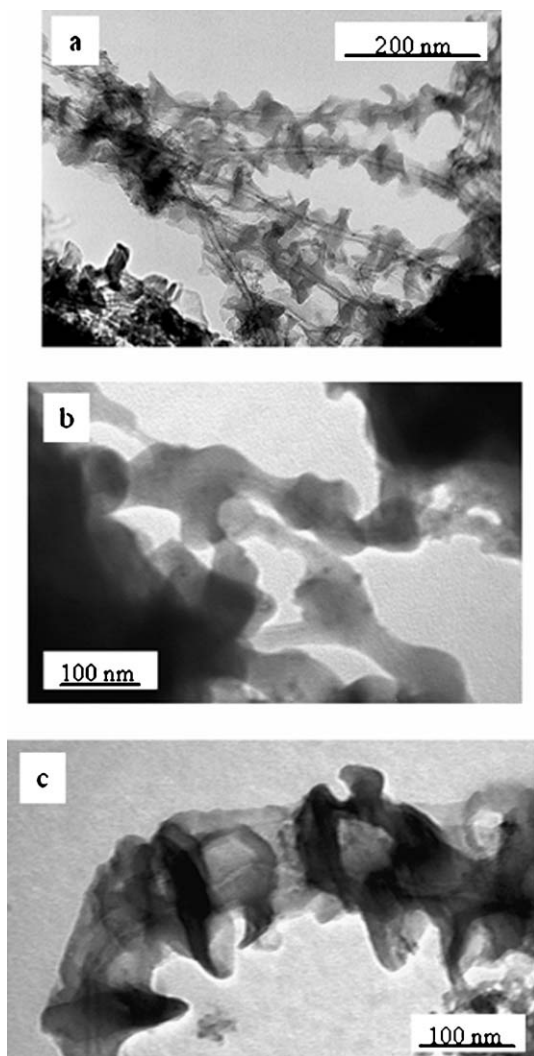


Fig. 6 TEM micrograph of PE-coated MWNT by the polymerization-filling technique at 0 (a), 40 (b) and 50 $^{\circ}\text{C}$ (c) respectively (see Table 2).

evident that the PE-coated MWNTs are completely separated from the starting bundle-like associations.

Conclusions

In conclusion, we have demonstrated that the polymerization-filling technique (PFT) can be used to synthesize polyethylene-carbon nanotube nanocomposite materials. The studies of the

nanotube-PE composites clearly indicate that multiwalled carbon nanotube treatment by PFT leads to the immobilization of methylaluminoxane as well as the subsequently added catalyst (*i.e.*, Cp^*ZrCl_2) onto the surface of the carbon nanotubes by electrostatic interactions as evidenced by SEM (EDS coupled), XPS and TOF-SIMS. The *in situ* polymerization of ethylene catalyzed by the active anchored metallocene complex proved to be fast and leads to the coating of the carbon nanotubes by the *in situ* grown polyethylene chains and precipitation of PE onto the nanotubes. Depending on the cocatalyst employed (MAO or MMAO-3A), the MWNTs are covered homogeneously or not (*i.e.*, PE/MWNT nanohybrid “sausage”-like or “shish-kebab”-like structures, respectively). Therefore, the type of coating morphology can be readily controlled by tuning the experimental conditions. As a result, the native carbon nanotube aggregates are isolated in comparison with the starting bundle-like associations, as confirmed by TEM analysis. Such deaggregation of the nanotubes is desired to get a truly nanocomposite structure with improved properties, and interestingly enough, preliminary results have shown that such PE-coated MWNTs, as obtained by PFT, could be homogeneously dispersed in various matrices (*e.g.*, HDPE¹⁸ or EVA²⁸) when melt blended leading to a significant improvement of the properties for the obtained materials in terms of mechanical properties (enhancement of stiffness). Such a coating involves only weak physical bonding, avoiding covalent modification, which should preserve the unique electrical and mechanical properties of the nanotubes. Moreover the difference in the coating morphology of the two series of prepared nanocomposites is expected to affect their macroscopic properties, particularly their electrical conductivity; these properties are under current investigation.

Acknowledgements

The authors thank Nanocyl S.A. (Sambreville, Belgium) for kindly providing the carbon nanotubes. We are grateful to Prof. M. Hecq and Dr R. Gouttebaron (Inorganic and Analytical Chemistry, UMH) for XPS and TOF-SIMS. This work was financially supported by “Région Wallonne” and the European Community (FEDER, FSE) within the framework of “Objectif 1: Materia Nova”. The Laboratory of Polymeric and Composite Materials thanks the “Belgian Federal Government Office Policy of Science (SSTC)” for general support in the frame of the PAI-5/03. S. B. thanks the “European Community” for financial support in the frame of the Nanohybrid project (STREP NMP3-CT-2005-516972).

References

- 1 S. Ijima, *Nature*, 1991, **354**, 56.
- 2 M. M. J. Treacy, T. W. Ebbesen and J. M. Gibson, *Nature*, 1996, **381**, 678.
- 3 E. W. Wong, P. E. Sheehan and C. M. Lieber, *Science*, 1997, **277**, 1971.
- 4 R. H. J. Baughman, A. A. Zakhidov and W. A. de Heer, *Science*, 2002, **297**, 787.
- 5 E. T. Thostenton, Z. Ren and T. Chou, *Compos. Sci. Technol.*, 2001, **61**, 1899.
- 6 R. Andrews and M. C. Weisenberger, *Curr. Opin. Solid State Mater. Sci.*, 2004, **8**, 31.
- 7 K. T. Lau and D. Hui, *Compos. Part B*, 2002, **33**, 263.
- 8 H. J. Lee, S. J. Oh, J. Y. Choi, J. W. Kim, J. Han, L. S. Tan and J. B. Baek, *Chem. Mater.*, 2005, **17**, 5057.
- 9 X. Gong, J. Liu, S. Baskaran, R. D. Voise and J. S. Young, *Chem. Mater.*, 2000, **12**, 1049.
- 10 M. S. Schaffer and A. H. Windle, *Adv. Mater.*, 1999, **11**, 937.
- 11 C. Park, Z. Ounaies, K. A. Watson, R. E. Crooks, J. Smith, S.E. Lowther, J. W. Connell, E. J. Siochi, J. S. Harrison and T. L. St. Clair, *Chem. Phys. Lett.*, 2002, **364**, 303.
- 12 C. A. Martin, J. K. W. Sandler, A. H. Windle, M.-K. Schwarz, W. Bauhofer, K. Schulte and M. S. P. Schaffer, *Polymer*, 2005, **46**, 877.
- 13 D. L. Shi, P. He, J. Lian, X. Chaud, S. L. Bud'ko, L. Beaugnon, M. L. Wang, R. C. Ewing and R. Tournier, *J. Appl. Phys.*, 2005, **97**, 064312.
- 14 D. L. Shi, J. Lian, P. He, L. M. Wang, F. Xiao, L. Yiang, M. J. Schultz and D. B. Mast, *Appl. Phys. Lett.*, 2003, **83**, 5301.
- 15 M. Olek, K. Kempa, S. Jurga and M. Giersig, *Langmuir*, 2005, **7**, 3146.
- 16 A. Star, J. F. Stoddart, D. Steurman, M. Diehl, A. Boukai, E. W. Wong, X. Yang, S.-W. Chung, H. Choi and J. R. Heath, *Angew. Chem., Int. Ed.*, 2001, **40**, 1721.
- 17 S. Bhattacharyya, C. Sinturel, J. P. Salvetat and M. L. Saboungi, *Appl. Phys. Lett.*, 2005, **11**, 113104.
- 18 D. Bonduel, M. Mainil, M. Alexandre, F. Monteverde and P. Dubois, *Chem. Commun.*, 2005, 781.
- 19 N. S. Enikolopian, *USSR Pat.*, 1976, 763 379.
- 20 E. G. Howard, *US Pat.*, 1978, 4 097 447.
- 21 W. Kaminsky and H. Zielonka, *Polym. Adv. Technol.*, 1993, **4**, 415.
- 22 M. Alexandre, E. Martin, P. Dubois, M. Garcia-Marti and R. Jérôme, *Macromol. Rapid Commun.*, 2000, **21**, 931.
- 23 M. Alexandre, E. Martin, P. Dubois, M. Garcia-Marti and R. Jérôme, *Chem. Mater.*, 2001, **13**, 236.
- 24 M. Alexandre, P. Pluta, P. Dubois and R. Jérôme, *Macromol. Chem. Phys.*, 2001, **202**, 2239.
- 25 A. Funck and W. Kaminsky, *Compos. Sci. Technol.*, 2007, **67**, 906.
- 26 J.-P. Trotignon, J. Verdu, A. Dobracinski and M. Piperaud, *Précis Matières Plastiques*, AFNOR/Nathan, Paris, 1996, p. 53.
- 27 L. Valentini, J. Bagiotti, M. A. Lopez-Machado, S. Santucci and J. M. Kenry, *Polym. Eng. Sci.*, 2004, **44**, 303.
- 28 S. Peeterbroeck, B. Lepoittevin, E. Pollet, S. Benali, C. Broekart, M. Alexandre, D. Bonduel, P. Viville, R. Lazzaroni and P. Dubois, *Polym. Eng. Sci.*, 2006, 1022.
- 29 M. Alexandre, P. Dubois, T. Sun, J. M. Garces and R. Jérôme, *Polymer*, 2002, **43**, 2123.
- 30 L. Li, C. Y. Li and C. Ni, *J. Am. Chem. Soc.*, 2006, **128**, 1692.